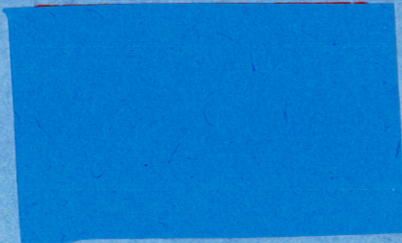


Investigation of Cryogenic Stability
and
Reliability of Operation of Nb₃Sn Coils
in
Helium Gas Environment

A.P. Martinelli, S.L. Wipf

IPP 4/100

July 1972



MAX-PLANCK-INSTITUT FÜR PLASMAPHYSIK

GARCHING BEI MÜNCHEN

MAX-PLANCK-INSTITUT FÜR PLASMAPHYSIK
GARCHING BEI MÜNCHEN

Investigation of Cryogenic Stability
and
Reliability of Operation of Nb₃Sn Coils
in
Helium Gas Environment

A.P. Martinelli, S.L. Wipf

IPP 4/100

July 1972

This paper was presented at the
"1972 Applied Superconductivity Conference",
Annapolis, Maryland, USA,
May 1 - 3, 1972.

*Die nachstehende Arbeit wurde im Rahmen des Vertrages zwischen dem
Max-Planck-Institut für Plasmaphysik und der Europäischen Atomgemeinschaft über die
Zusammenarbeit auf dem Gebiete der Plasmaphysik durchgeführt.*

INVESTIGATION OF CRYOGENIC STABILITY AND RELIABILITY
OF OPERATION OF Nb₃Sn COILS IN HELIUM GAS ENVIRONMENT

A. P. Martinelli and S. L. Wipf
Max-Planck-Institut für Plasmaphysik
8046 Garching / Munich, W. Germany

SUMMARY

The optimum operating temperature of coils with regard to economy of refrigeration and price of superconductor is above 4.2°K. The performance of Nb₃Sn coils made of 2, 4, and 8 pancakes (ID 22 cm, OD 32 cm, tape width 0.5 cm) was tested in the 4.2 - 17°K range. The cryogenic stability limit is calculated in liquid helium to be 90 A and is measured to be 70 A in gas at 4.2°K, dropping to about 20 A when T approaches T_C. Above these current limits, i.e. in the metastable range, the coils were tested for their response to local heating, which was applied in steady state (isothermal disturbance) or as a pulse (adiabatic disturbance) of increasing power until quench occurs. A model of the coil response to local heating is developed and compared with the experimental results.

INTRODUCTION

The reason for this study is twofold:
1. In the construction and use of Nb₃Sn coils for a levitated multipole experiment to be operated up to 15°K, the stability of these coils to thermal disturbances is of interest.¹
2. Economic considerations give an optimal operation temperature for superconducting coils, determined by the cost of the superconductor and the cost of the refrigerator which respectively increases and decreases with temperature. Calculation gives such temperatures as around 6-11°K, depending on the size of the coils, etc.

In Fig. 1 the results of a cost calculation for a coil system such as might be used in a large stellarator ("W7", about 60 MJ stored energy²) are presented. The hatched area between curves s and s₂ gives the present Nb₃Sn superconductor cost of the W7 coil system on the assumption that no coil degradation takes place. Curves s and s₂ differ by a factor of 2 owing to the difference in price quoted by various manufacturers. Curve d represents the superconductor cost of W7 by assuming the same coil degradation experienced by the 8-pancake test coil shown in Fig. 2.¹ The "degraded" curve d corresponds to the "short sample" curve s. The 1 kW refrigerator costs, expressed by curve r, are taken from Winters and Snow³ and are found to coincide approximately with the price set by recent competitive offers made by several European firms.

The sum of the capital costs of refrigerator and superconductor (r + s, and r + d for the degraded coil system) shows a minimum around 6°K. It is, how-

ever, anticipated that the superconductor prices might drop one order of magnitude in the future when very large quantities will be manufactured and marketed. With the superconductor price reduced to 1/10, the resulting new cost curves (r + s/10, and r + d/10) show a minimum between 10 and 11°K. In this case, operation at this temperature would allow a saving in capital costs of superconductor and refrigerator of about 35% in comparison with operation at 4.2°K.

So far operation of coils other than in liquid helium is not standard. Only very small coils are known to have been operated in helium gas at temperatures higher than 4.2°K and in a magnetic field contributed to a minor extent by the coil self-field and to a major extent by the background field of a larger coil^{4,5}. The present study concerns the response of coils to heat released within their windings, covering the temperature range between 4.2°K and T_C.

The results are of more general interest in connection with coils cooled by supercritical helium⁶ and the operation of coils, made of Nb-Ti as well as of Nb₃Sn, in the metastable regime. Large coils, especially, have sources of sudden heat release by friction, mechanical deformation or cracking; continuous heat sources can be joints and weak spots in the superconductor. Experiments on the release of heat in the windings of large coils have often been done, as part of the coil testing procedure.⁷⁻⁹

EXPERIMENTAL

Coils were made of 0.5 cm wide Nb₃Sn tape (GE; stainless steel reinforced,

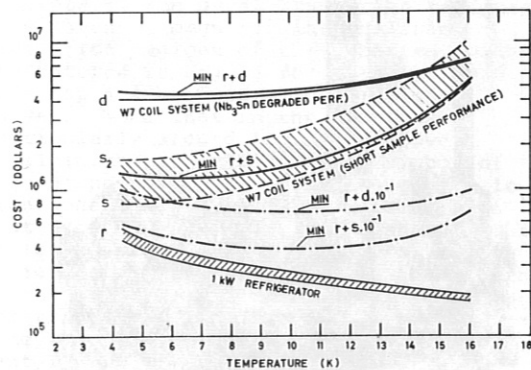


Fig. 1 Capital costs of 1 kW refrigerator and Nb₃Sn coil system for a large stellarator experiment (W7) as a function of temperature.

short sample ratings between 300 and 500A at 60 kG and 4.2°K) wound into pancakes of ID 22 cm, OD 32 cm, and 250 turns each. They were mounted with slotted anodized aluminum spacers of 0.2 cm thickness and energized by two pairs of current leads each to 4 pancakes in series. This allowed operation of all 8 in series, of 4 only in series, or 4 and 4 in opposition (cusp configuration). Fig. 2 shows a picture of the coil assembly. Some measurements were also made on a smaller coil consisting of 4 pancakes wound with aluminum tape of 30 μ and 50 μ thickness interleaved between the winding turns; this coil was operated in cusp configuration.¹ A more detailed description of the two coils is given in the previous paper.¹

Several heaters were made of flattened constantan wire between two mylar foils; they have the width of the tape and are 3 cm long and 80 μ thick. They are located as follows; at the centre of the winding of one of the two middle pancakes, i.e. between turns 125 and 126 ("white" heater in the 8-pancake coil, "red" heater in the 4-pancake coil); in the adjacent outer pancake, also at the centre of the winding ("green heater in the 4-pancake coil) or about 1/3 along the winding starting from the inner winding border, i.e. between turns

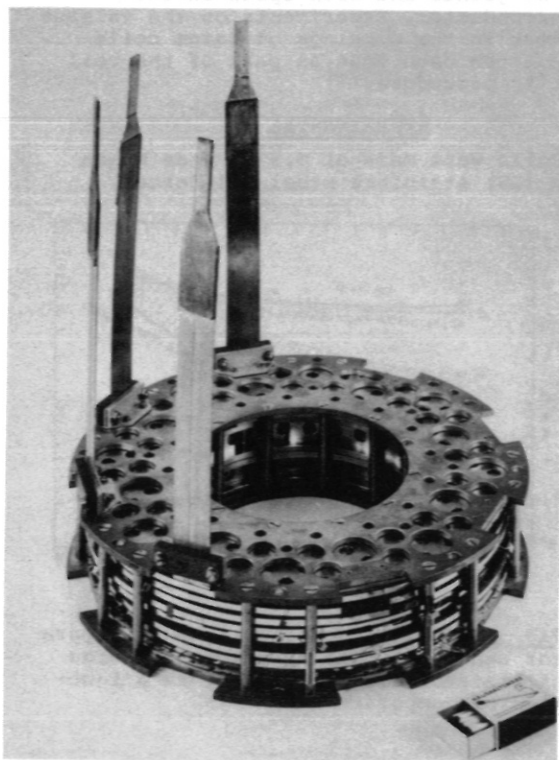


Fig. 2 Eight-pancake coil.

80 and 81 ("red" heater in the 8-pancake coil). The heater current used had both a rectangular shape (0.5 s minimum duration) obtained by switching on and off a d.c. power supply, and a trapezoidal shape (see Fig. 6) obtained by a motor driven power supply.

As thermometers, 14 carbon resistors were distributed throughout the larger coil, and 10 in the smaller coils. They were located between the pancakes in the slots of the Al spacers. The temperature in the cryostat was adequately controlled (to $\pm 0.1^\circ\text{K}$ for approximately 10 min) by regulating the transfer rate of helium from a liquid container and the power of a heater at the bottom of the cryostat.

MEASURING PROCEDURE AND RESULTS

Two of the three variables I (coil transport current), T_0 (coil temperature, and I_p (heater current) are set, the third is varied until quench occurs. Of interest are the power level and duration of heating which can be tolerated, or which just produce quench.

The response of the coil temperature to a heater current step gives an idea of the thermal diffusivity within the coil. It takes the temperature about 15 s to reach equilibrium within a heated zone (i.e. until a heated region is fully developed). The zone extends very rapidly along the winding around the whole coil, but much more slowly radially across the windings in the pancake, and most slowly laterally from pancake to pancake (see Fig. 6 pulse 2). In this sense one can distinguish short pulses of less than 10 s and long pulses of more than 10s.

Short survey and examples of performance

As a rule a heat pulse brings into play two more sources of heat: 1. It can trigger flux jumps (magnetic instabilities) which release magnetically stored energy as a spatially extended adiabatic heat pulse. 2. It creates a normal zone in which ohmic heating ρj^2 is released as long as the zone can exist. Here ρ is the resistivity in the normal state and j the current density, both averaged over the total cross section of the winding.

Fig. 3 shows examples of the response of the carbon thermometer next to the heater and the change in coil terminal voltage, (which is interpreted as resistance) due to a series of increasing adiabatic pulses (0.5 s duration). In one case a quench is obtained, in the other the coil remains superconductive up to the highest pulses of $Q_a = 18 \text{ J}$.

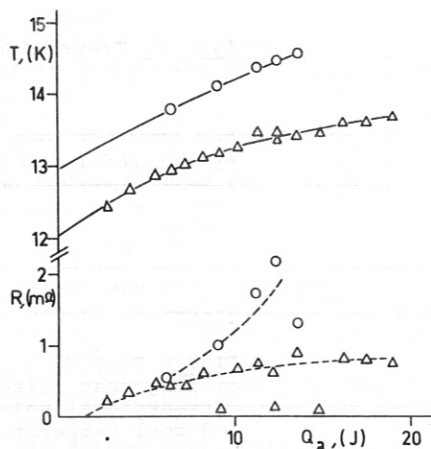


Fig. 3 Temperature and resistance response as a function of heat released during pulses of 0.5 s duration for cusp 4-4 coil configuration.

Stable situation: (Δ): coil at 12 $^{\circ}$ K, 45 A
 Unstable situat: (o): coil at 13 $^{\circ}$ K, 50 A
 (transition for $Q_a = 18$ J)

Fig. 4 gives a survey and examples of results of 2 measuring procedures which were used: a) A constant heater current I_p was established and the coil current I increased from zero up to coil quench; b) from a preset (I, T_0) point the heater current was increased from zero (either continuously or in successive pulses) up to coil quench. Procedure b) is applied in example A, with the succession of heat pulses indicated. In this fashion, the loci of (I, T_0) points which can withstand pulses of 1, 5, 10 J were obtained. Near the stability boundary (curve STABLE) pulses larger than 25 J are needed to produce a quench (burning-out power of heater $\dot{Q} \approx 80$ W). Procedure a) is used to test the cryogenic stability limit with the coil in liquid helium (see example B). The results are 75-95 A, depending on the heater power, which compares with a calculated limit of 90 A. In gas, both type a) (see example C) and type b) tests (see example D) give transitions close to the usual transition range. The transition is preceded by a resistive region and is then given by a thermal runaway of the ohmic heating. The amount of ohmic heating under runaway conditions is indicated in example B and C as 2 and 1.4 W respectively. Resistive regions are observed in the hatched area of Fig. 4, which is similar to a current sharing regime because the resistive zone is steady.

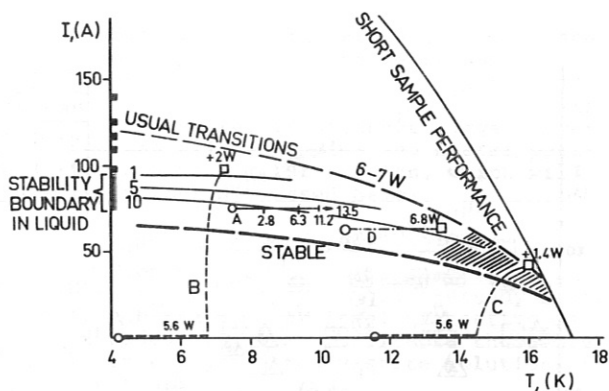


Fig. 4 Stability regions (cusp 4-4 coil configuration; heater at B_r max). In the metastable region are three curves below which the coil can tolerate 0.5 s pulses of 1, 5, 10 J, without going normal. Examples of responses to various experimental conditions:

- A. Short pulses (0.5 s) at constant coil current. Quench at 13 J.
- B. Isothermal heating, const. 5.6 W, steady increase of coil current, coil in liquid helium.
- C. Same as B, coil at 11.5 $^{\circ}$ K.
- D. Constant current, increase heating until quench (at 6.8 W).

Results of short heat pulses

Fig. 5 illustrates all the transitions experienced by the 8-pancake coil subjected to short heat pulses. Three regimes can in general be distinguished. First, where the quenches are governed by magnetic instabilities. This region is close to the usual transition regions also given by magnetic instabilities.¹ Transition regions of the unheated coil are entered in Fig. 5 for both series 8 and cusp 4-4 configurations (hatched curves). Note that in the cusp case, particularly around 100 A, the power level (number entered in each symbol of Fig. 5) necessary to produce a quench is about one order of magnitude lower than that necessary to produce a quench in the series case. This is ascribed to the magnetic instabilities induced in the windings by the high value of the radial field B_r for the cusp configuration.¹ A second regime is observed at lower transport current I in which the quench takes place mainly because of runaway due to ohmic heating of the normal zone initiated by the heat pulse. A third regime of relative coil stability is found at still lower currents and temperatures. Here the difference between series and cusp configuration is very small, and a high power level is necessary to cause transition.

The general scatter of points is large.

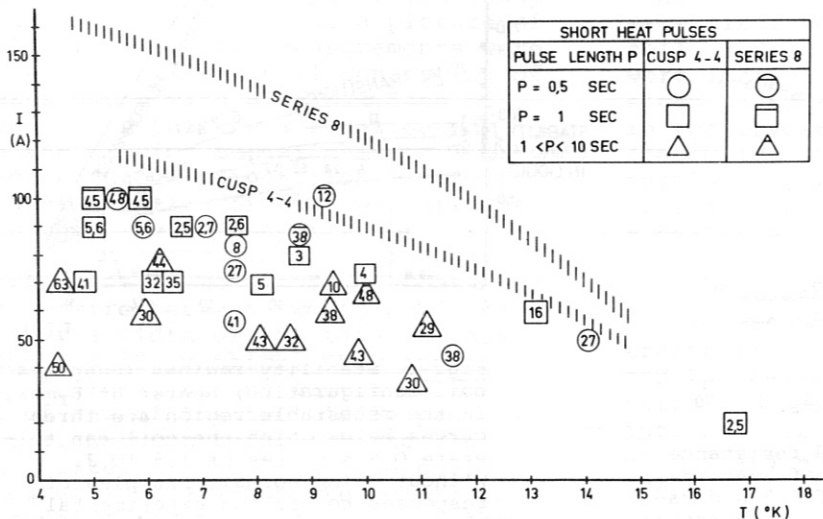


Fig. 5. Transitions caused by short heat pulses in the 8-pancake coils. The number given in each symbol refers to the lowest observed power level leading to a quench.

BELOW

Fig. 6 Recordings of long heat pulse current, coil voltage and coil temperature versus time.

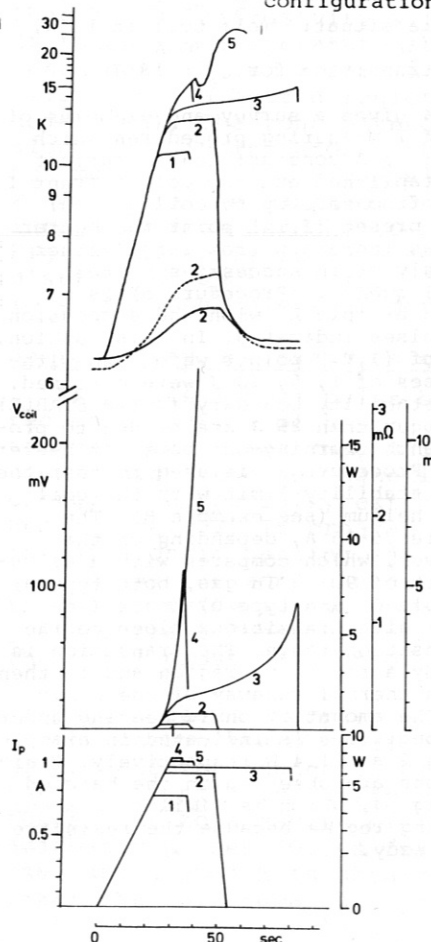
("green" heater in the aluminum stabilized coil with transport current I=75 A, 2-2 cusp configuration.)

Besides the usual scattering factors (flux jumps, training) it should be noted here that a major scattering factor is due to the fact that the observed power level necessary to quench may be up to 20% higher than the minimum power level necessary because of the increase of the pulse power by steps of about this size. A further reason for scattering of short pulse data is discussed below.

It is the second and third regions in which the thermal conditions (cooling, heat conduction, and diffusivity or specific heat) of the coil are of dominating importance. These regions are studied in more detail by means of long pulses.

Results of long heat pulses

Fig. 6 gives an example of transition due to a long pulse. The response to five pulse profiles of different height and duration is illustrated. Pulse 1 only just produces a normal zone, as the resistance shows. During pulse 2 the normal zone is larger, but steady in time. For pulse 2 the temperature profile is shown not only for the thermometer close to the heater (green) as in pulse 1-5 but also for the thermometers which are still near the pancakes away from the heater, but one (dotted) and two pancakes away in the axial direction of the coil. Notice the lag of more than 10 s in establishing the temperature plateau and also the falling off of the temperature across the coil transversely to the pancakes. A similar falling off is observed radially along the pancake inwards and outwards from the heater. In contrast, along the windings adjacent to the heater the hot zone extends right around the coil; 180° opposite the heater



the temperature excursion is still about 50% (extensive temperature profiles within the coils have been measured but are not shown).

During pulse 3 the normal zone is even larger. If a heat pulse lasts long enough the zone will grow and a quench will develop. This is largely because the primitive temperature control system cannot keep the temperature T_0 constant in the long run against the increased heating of heater and ohmic heating. The heater pulse 4 exceeds the quench power, but it is switched off again before the quench can develop. Pulse 5 causes quench. The temperature profile indicated that by the time the heater is switched off the normal zone is so far extended that its ohmic heating soon raises the coil substantially above the transition temperature. In these cases the coil power supply is switched off. Additional scales give the heater power and the power in the resistive region ($j^2 \rho$, volume) and also the total resistance and the total length of tape affected in the resistive region, (using the measured value of $2.7 \mu\Omega/\text{cm}$ normal tape).

Fig. 7 gives results of transitions achieved with long pulses. As in Fig. 5 the lowest observed power levels which cause a transition within a short time (≈ 10 s) are entered in each symbol.

Also entered in this figure are the usual transition regions of the unheated 8-pancake coil in the various geometries. On the right-hand side there is a scale of $j^2 \rho$, j and ρ being average values of the current density and resistivity within the coil windings. Curves of constant

stability parameter are also given (see below), $\xi = 0$ being the short sample curve.

The scatter is no doubt large. Nevertheless all geometries and heater positions give similar results, which will be further discussed below.

ANALYSIS AND DISCUSSION

From Fig. 6 it can be seen that quenches develop from quasi-steady states if a certain power level of heating is exceeded. It seems profitable therefore to investigate steady-state solutions to the thermal problem.

As a first approximation a coil winding extending to infinity in all directions is assumed with an isotropic thermal conductivity k . Spherical coordinates are taken and the heater with power \dot{Q} is placed within a small space $\langle r_0$ around the origin. A normal zone is assumed to exist for $0 < r < R$ where the temperature $T > T_1$ and the heat production $\dot{q} = j^2 \rho$ ($T_1 =$ critical temperature for current density j).

Outside R the winding remains superconducting; for $r > R$, $\dot{q} = 0$.

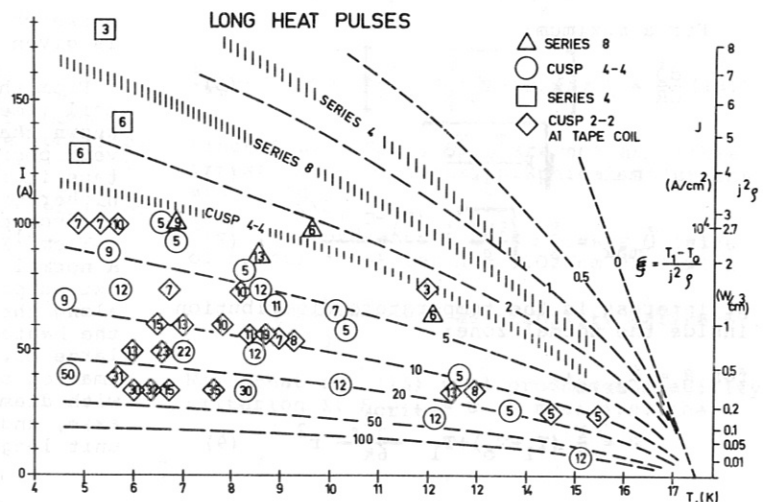
Boundary conditions: when $r = R$, $T(R) = T_1$; for $r \rightarrow \infty$, $T \rightarrow T_0$; for $r > R$ the heat flux F is constant:

$$F = -k(dT/dr)4\pi r^2. \quad (1)$$

Hence integrating and applying both boundary conditions:

$$T = (T_1 - T_0)(R/r) + T_0 \quad (2)$$

Fig. 7 Quench points obtained with heat pulses longer than 10 s for the two coils and different configurations indicated.



and at $r = R$

$$F(R) = k(T_1 - T_0) 4\pi R. \quad (3)$$

This heat flux must equal the heat produced within the sphere

$$F(R) = k(T_1 - T_0) 4\pi R = \frac{4}{3}\pi R^3 j^2 \rho + \dot{Q}$$

so $\dot{Q} = 4\pi R \left[k(T_1 - T_0) - \frac{1}{3} j^2 \rho R^2 \right] \quad (4)$

when $\dot{Q} = 0$

$$R_{crit} = \sqrt{3k \frac{T_1 - T_0}{j^2 \rho}} \quad (5)$$

For $R < R_{crit}$ the normal zone collapses and for $R > R_{crit}$ it grows by itself without any heater power.

A short pulse would have to be large enough to create a zone of the size $r = R_{crit}$ in order to cause a transition. The enthalpy of the zone gives a rough estimate of the necessary energy required. Solutions of an unsteady temperature distribution give a more accurate picture (see ref. 10, Fig. 4); the accurate solution is further complicated by the $j^2 \rho$ term and the energy released by flux jumps. The very slow growth of a normal zone can be represented by passing through a continuous series of steady states. The necessary heater power to maintain a zone smaller than R_{crit} is given by eq. (4). \dot{Q} passes through a maximum at R_{max} . (Once $r > R_{max}$ the zone cannot be in stable equilibrium.) For $\dot{Q} > \dot{Q}_{max}$ the zone will grow. Thus \dot{Q}_{max} gives the necessary heater power to create a quench. However, if the heater power is switched off after the zone has started to grow beyond R_{max} but before it has reached R_{crit} it will collapse again. This may be the cause for much scattering in the short pulse data, as in Fig. 5. (See also pulses 4 and 5 in Fig. 6.)

For a maximum:

$$\frac{d\dot{Q}}{dR} = 4\pi \left[k(T_1 - T_0) - R^2 j^2 \rho \right] = 0 \quad (6)$$

$$R_{max} = \sqrt{k \frac{T_1 - T_0}{j^2 \rho}} \quad (7)$$

$$\dot{Q}_{max} = \frac{8}{3}\pi \sqrt{\frac{k^3}{\rho}} \cdot \frac{(T_1 - T_0)^{3/2}}{j} \quad (8)$$

Of interest is the temperature distribution inside the normal zone:

for $R = R_{crit}$:

$$T = \frac{1}{2} (T_1 - T_0) + T_1 - \frac{j^2 \rho}{6k} r^2 \quad (9)$$

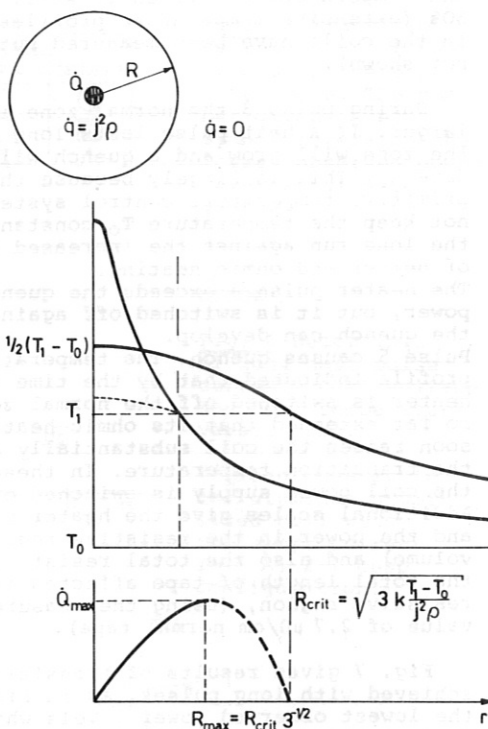


Fig. 8 Spherical approximation of coil winding.

and $T_{max} = T_1 + \frac{1}{2}(T_1 - T_0)$ at $r = 0$;

for $R < R_{crit}$:

$$T = T_1 + \frac{j^2 \rho}{6k} (R^2 - r^2) + \frac{\dot{Q}}{4\pi k} \left(\frac{1}{r} - \frac{1}{R} \right) \quad (10)$$

A sketch of the spherical approximation is given in Fig. 8.

From the temperature profile in the coil (see discussion of Fig. 6) it is known that the spherical approximation is very poor. In reality the k along the tape is about two orders of magnitude higher than the k normal to the windings or from pancake to pancake (k of Cu $\approx 1 \text{ W cm}^{-1} \text{ K}^{-1}$; k of stainless steel ≈ 0.01). A normal zone created by the heater will extend practically around the whole coil, along the tape in immediate contact with the heater. Assuming a sufficiently large coil radius one can make the approximation of a cylindrical normal zone with diameter $2S$, which is heated on the axis, and calculate the heat flux per unit length (Fig. 9).

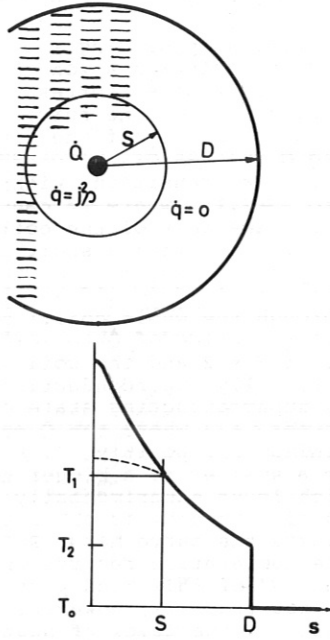


Fig. 9 Cylindrical approximation of coil winding.

Similar to the spherical case:

for $s < S$, $T > T_1$ and $\dot{q} = j^2 \rho$

for $s > S$, $T < T_1$ and $\dot{q} = 0$

The heat flux equation corresponding to eq. (1) for $s > S$ is

$$F = -k \frac{dT}{ds} 2\pi s \quad (11)$$

which is integrated to yield

$$T = \frac{F}{2\pi k} (B - \log s).$$

The boundary conditions determine constants F and B. The assumption of an infinite body with $T(s \rightarrow \infty) = T_0$ does not have a solution, unlike the spherical case. Instead the body is assumed to have a surface at $s = D$ with a surface temperature T_2 and a heat transfer coefficient h. Then the constants become:

$$F = \frac{k 2 \pi T_1}{B - \log S} = \frac{k 2 \pi T_2}{B - \log D} \quad \text{with}$$

$$B = \frac{T_1 \log D - T_2 \log S}{T_1 - T_2}$$

and eqs. (12) to (18) correspond to eqs. (2) to (8) of the spherical case.

$$T = (T_1 \log \frac{D}{S} + T_2 \log \frac{S}{S}) / \log \frac{D}{S} \quad (12)$$

When $s = S$ the heat flux is given by

$$h(T_2 - T_0) 2\pi D = 2\pi \frac{k(T_1 - T_2)}{\log \frac{D}{S}} = j^2 \rho \pi S^2 + \frac{\dot{Q}}{L} \quad (13)$$

L being the total length of the cylindrical normal zone.

Elimination of

$$T_2 = \left(T_0 + \frac{k T_1}{h D \log \frac{D}{S}} \right) / \left(\frac{k}{h D \log \frac{D}{S}} + 1 \right)$$

gives

$$\dot{Q} = L 2\pi \left(\frac{k(T_1 - T_0)}{\log \frac{D}{S} + \frac{k}{h D}} - \frac{1}{2} j^2 \rho S^2 \right). \quad (14)$$

$\dot{Q} = 0$ for

$$S_{\text{crit}} = \sqrt{2k \frac{(T_1 - T_0)}{j^2 \rho \left(\log \frac{D}{S_{\text{crit}}} + \frac{k}{h D} \right)}}. \quad (15)$$

The maximum heater power is determined by

$$\frac{d\dot{Q}}{dS} = 2\pi L \left[\frac{k(T_1 - T_0)}{S \left(\frac{k}{h D} + \log \frac{D}{S} \right)^2} - j^2 \rho S \right] = 0 \quad (16)$$

$$S_{\text{max}}^2 \left(\frac{k}{h D} + \log \frac{D}{S_{\text{max}}} \right)^2 = k \xi \quad (17)$$

$$\text{with } \xi = \frac{T_1 - T_0}{j^2 \rho}.$$

$$\dot{Q}_{\text{max}} = 2\pi L j^2 \rho S_{\text{max}} \left(\sqrt{k \xi} - \frac{1}{2} S_{\text{max}} \right). \quad (18)$$

Since S_{crit} , S_{max} , \dot{Q}_{max} are not available in explicit solutions, graphical solutions are given.

Fig. 10 represents $\dot{Q}/L j^2 \rho$ versus S (size of normal zone) for $k = 0.02 \text{ Wcm}^{-1} \text{K}^{-1}$ with

$$\xi = \frac{T_1 - T_0}{j^2 \rho} \quad \text{as stability parameter.}$$

Note that eq. (15) will produce a stability criterion if $S_{\text{crit}} = D$ is set; i.e. the

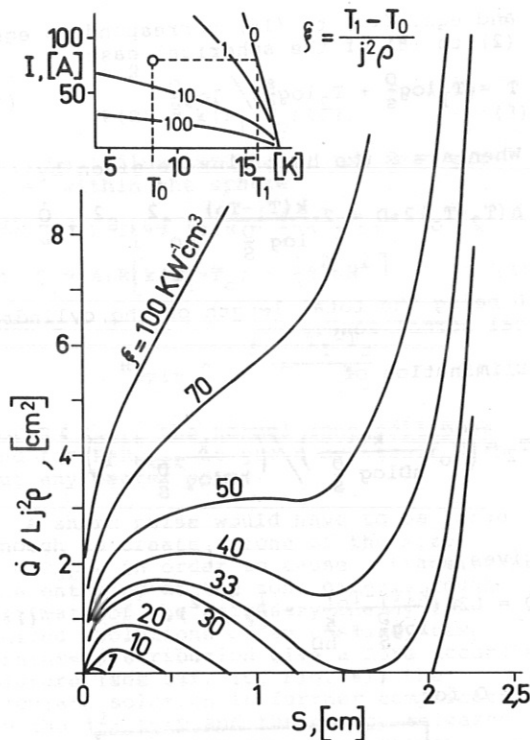


Fig. 10 $\dot{Q}/Lj^2\rho$ versus S (size of normal zone) for $k = 0.02 \text{ Wcm}^{-1}\text{K}^{-1}$ with ξ as stability parameter, and $h = 0.1 \text{ Wcm}^{-2}\text{K}^{-1}$, $D = 2.5 \text{ cm}$.

cooling at the surface will remove, at least for a short time, the ohmic heating produced in the coil when all of it is normal and, therefore, the surface temperature $T_2 = T_1$. This is rather similar to the stability criterion in liquid helium, where the peak nucleate boiling should be capable of keeping the fully normal conductor below about 5°K (also for a limited time only).

The criterion gives $D^2 = 2\xi hD$,

$$\xi = \frac{D}{2h} \quad (19)$$

Choosing $h = 0.1 \text{ Wcm}^{-2}\text{K}^{-1}$ (in reality it may be 2-5 times smaller, but the order of magnitude is correct) and $D = 2.5 \text{ cm}$, we expect stable performance for $\xi > 12.5 \text{ Kcm}^2\text{W}^{-1}$ irrespective of k .

Fig. 10 shows a much more complicated situation. Taking $\xi = 10$ (unstable situation) $\dot{Q}(S)$ behaves as in the spherical case, going through a maximum at $S \approx 0.2 \text{ cm}$ and reaching zero at $S_{\text{crit}} = 0.45$. Beyond, the zone will grow until the whole coil is normal. Taking the curve

for $\xi = 30$ there is a difference: beyond $S_{\text{crit}} = 1.2 \text{ cm}$, the zone will also grow, but will stop growing when $S \approx 2 \text{ cm}$ is reached. To maintain a zone $S > 2 \text{ cm}$ requires a heater power corresponding to the ascending part of the curve. Looking at a quenching experiment one finds on increasing \dot{Q} that at \dot{Q}_{max} (for $S \approx 0.45 \text{ cm}$) there will be a transition, with the zone growing to $S \approx 2.15$, where it can remain stable, with the rest of the coil still superconducting. (After a short time in this state the cooling medium would warm up and the transition would eventually spread through the whole coil.) With subsequent reduction of \dot{Q} to zero the zone will stay at $S = 2$ and the coil will not recover its fully superconducting state. The fully superconducting state can be recovered for $\xi \geq 33$ where the \dot{Q} curves show a minimum for positive \dot{Q} . A transition from a smaller to a bigger normal zone, which looks experimentally like the beginning of a quench, is observed up to $\xi = 50$, where the curve has a saddle point. The temperature records show that for "quenches" of this kind part of the coil does not reach T_1 ; however, after the transition, the level of heating is normally so high that the coil warms up rapidly and normalizes.

By way of summary, one can state that the analysis shows for $\xi \leq 12.5$ full instability (i.e. a full quench for $\dot{Q} > \dot{Q}_{\text{max}}$); for $12.5 < \xi < 33$ a transition which cannot recover (i.e. the coil does not become fully normal, but cannot recover the fully superconducting state); for $33 < \xi < 50$ a transition which can recover (i.e. for $\dot{Q} \rightarrow 0$ the coil becomes fully superconducting again); finally, for $\xi > 50$ one obtains full stability (i.e. a normal zone grows with increasing \dot{Q} until the coil is normal, but there are no thermal runaway transitions).

It should be pointed out that all curves reach finite values at $S = D = 2.5 \text{ cm}$. These values are given by $\dot{Q}/L = (T_1 - T_0)h2\pi D$

$$\text{or } \frac{\dot{Q}}{Lj^2\rho} = \xi h2\pi D \quad (20)$$

In the present experiments both h and D are poorly defined (h is almost certainly not constant). While the choice of h affects the curves shown in Fig. 10 near $S = D$, the value of k alters the picture for $S < D$.

To describe the situation for different k values $\dot{Q}_{\text{max}}/Lj^2\rho$ versus S_{max} is plotted in Fig. 11. As an indication of the instability boundary the value $\xi = 10$ is entered.

The curves terminate at the saddle point for which the value for ξ is given.

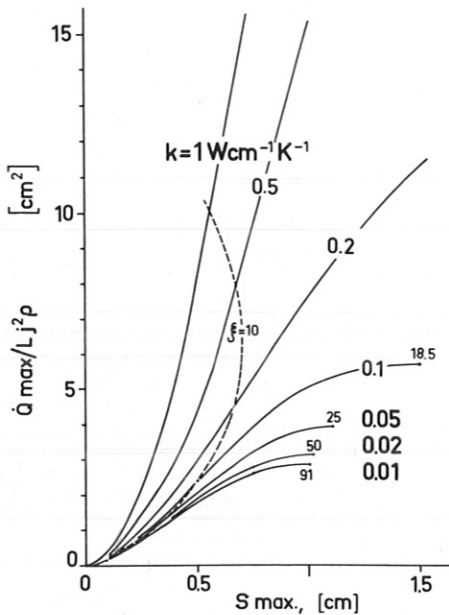


Fig. 11 $\dot{Q}_{\max}/Lj^2\rho$ vs S_{\max}

In Fig. 12 quenches (or transitions) for long pulses are entered for both coils, all geometries, and different heaters, as $\dot{Q}/j^2\rho$ versus ξ . A fit with the theory is attempted, whereby both k and L are, within reasonable limits, adjustable "effective" parameters. The red heater of the 4-pancake coil and the white heater should come closest to the approximations of the analysis, but the scatter is too large to show any definite trend. Considering the crudeness of the theory compared to the complex situation in a real coil, the fit is better than expected. An effective k of $0.03 \pm 0.02 \text{ Wcm}^{-1}\text{K}^{-1}$ seems reasonable, also an L of $30 \pm 20 \text{ cm}$.

CONCLUSIONS

- The analysis indicates a stability parameter $\xi = (T_1 - T_0)/j^2\rho$ as a measure of the degree of cryogenic stability of a coil.
- The stability limit is, in general, characterized by four different degrees: full instability, non-recoverable transition, recoverable transition, full stability.
- For good stability a high value of k is essential.
- The use of reinforcing steel tape bonded with superconducting tape apparently impairs performance. Also good

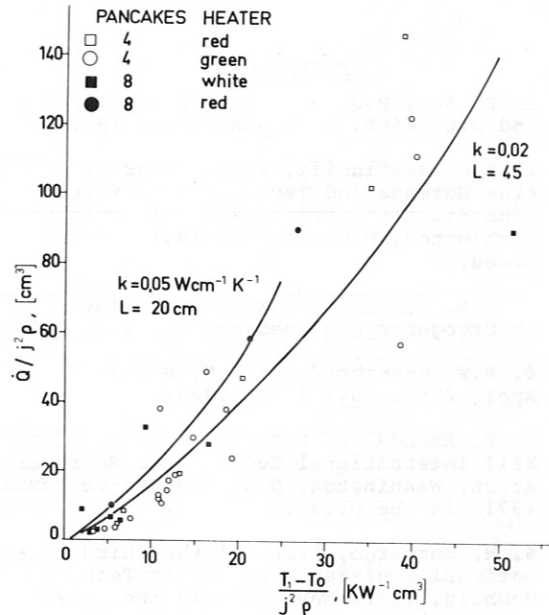


Fig. 12 Transitions for long pulses and for both coils and geometries, entered as $\dot{Q}/j^2\rho$ versus ξ .

thermal contact between pancakes should be ensured.

- Tolerable heater power levels can be fairly high.
- Operation in gas is as reliable as in liquid.
- Operation of coils at temperatures higher than 4.2°K is economically attractive, especially if superconductors with higher critical current density at temperatures higher than 4.2°K become available at a lower price.

ACKNOWLEDGMENTS

The authors are grateful to a number of colleagues for their support and providing of experimental facilities. Special thanks are due to Mrs. S. Wipf, for checking the mathematics.

This work was performed under the terms of the agreement on association between Max-Planck-Institut für Plasma-physik and EURATOM.

REFERENCES

1. F. Rau, H.J. Jäckel, A.P. Martinelli, and S.L. Wipf, ASC, Annapolis, 1972.
 2. A.P. Martinelli, Proceedings of "The Science and Technology of Superconductivity", Georgetown University, Washington, D.C., August 1971, in the press.
 3. A.R. Winters and W.A. Snow, Advances in Cryogenic Engineering, 11, 116, (1965)
 4. R.W. Meyerhoff and B.H. Heise, J. Appl. Phys., 36, 137, (1965).
 5. W. Amenda and A.P. Martinelli, Proc. XIII International Congress of Refrigeration, Washington, D.C., August-September 1971, in the press.
 6. M. Morpurgo, Proc. of the Third International Conference on Magnet Technology, Hamburg, 19-22 May 1970, in the press.
 7. Z.J.J. Stekly, E.J. Lucas, T. deWinter, B. Strauss, F. Di Salvo, J. Laurence, and W. Coles, J. Appl. Phys. 39, 2641 (1968).
- also
- Lucas et al. Adv. Cryog. Eng. 15, 167 (1970); J. Appl. Phys. 40, 2101 (1969).
8. C. Laverick, IEEE Spectrum 5, 63 (1968)
 9. L. Cesnak and J. Kokavec, Cryogenics 12, 116, (1972).
 10. H.S. Carslaw and J.C. Jaeger, "Conduction of Heats in Solids", (Oxford University Press, 1959), 2nd Ed., Chap. 2, p. 55.